JACS
JOURNAL OF THE AMERICAN CHEMICAL SOCIETY
Communication
pubs.acs.org/JACS

Irreversible Network Transformation in a Dynamic Porous Host Catalyzed by Sulfur Dioxide

Sihai Yang,*[,†] Leifeng Liu,[‡] Junliang Sun,[‡,§] K. Mark Thomas,[∥] Andrew J. Davies,[†] Michael W. George,[†] Alexander J. Blake,[†] Adrian H. Hill,[⊥,#] Andrew N. Fitch,[⊥] Chiu C. Tang,[¶] and Martin Schröder*[,†]

[†]School of Chemistry, University of Nottingham, University Park, Nottingham, NG7 2RD, U.K.

[‡]Department of Materials and Environmental Chemistry, Stockholm University, Stockholm, 10691, Sweden

[§]College of Chemistry and Molecular Engineering, Peking University, Beijing, 100871, China

[∥]Wolfson Northern Carbon Research Laboratories, School of Chemical Engineering and Advanced Materials, University of Newcastle upon Tyne, Newcastle upon Tyne, NE1 7RU, U.K.

[⊥]European Synchrotron Radiation Facility, Grenoble, 38043, France

[¶]Diamond Light Source, Harwell Science and Innovation Campus, Didcot, Oxfordshire, OX11 0DE, U.K.

Supporting Information

ABSTRACT: Porous NOTT-202a shows exceptionally high uptake of SO_2, 13.6 mmol g^{-1} (87.0 wt %) at 268 K and 1.0 bar, representing the highest value reported to date for a framework material. NOTT-202a undergoes a distinct irreversible framework phase transition upon SO_2 uptake at 268−283 K to give NOTT-202b which has enhanced stability due to the formation of strong $\pi\cdots\pi$ interactions between interpenetrated networks.

Studies on the adsorption of carbon dioxide (CO_2) by porous metal−organic framework (MOF) materials are attracting enormous interest because of their potential to capture CO_2 from flue gases.[1] MOFs often exhibit large internal surface areas and extended crystal structures, and their properties are thus amenable to study by advanced diffraction techniques.[2] An interesting feature is that CO_2 adsorption may trigger reversible phase changes in the host materials, leading to an increase in pore volume and enhanced CO_2 uptake.[3−11] These structural changes can disappear or become much less distinct when the MOF is exposed to other adsorbates such as N_2, CH_4, and H_2, which, unlike CO_2, possess small or zero quadrupole moments.[9,12,13] Framework flexibility can also involve changes in metal−ligand coordination geometry,[3,8,13] free rotation of side chains on the organic linker,[9,14] pore opening/closing mechanisms coupled to phenyl ring rotation,[12] gating of guest molecules,[15] or, as recently discovered, bulk structural defects.[16]

Although CO_2 adsorption in MOFs has been intensively studied, the capture and storage of SO_2[17,18] in MOFs have barely been reported.[19−21] SO_2 is highly corrosive, and few porous MOF materials are stable to the presence of SO_2. Even though the amount of SO_2 in the flue gas is much lower than that of CO_2, it still presents a significant environmental hazard, and the development of effective capture methods for SO_2 using highly stable MOFs represents a significant challenge. We report herein the highly selective adsorption of SO_2 by a dynamic material NOTT-202a in which a dramatic irreversible phase transition is observed upon adsorption of SO_2 into NOTT-202a at 268−283 K to form NOTT-202b. Overall, the phase change process, which does not occur with other gases, can be viewed as a chemical transformation catalyzed by acidic SO_2 gas with NOTT-202a being converted into NOTT-202b in near-quantitative yield.

NOTT-202a has a doubly interpenetrated framework structure but with one of the networks having only ∼75% occupancy due to the conflicting steric requirements of the ligands leading to a defect structure.[16] Each of the single networks is constructed from mononuclear $[In(O_2CR)_4]$ nodes bridged by L^{4-} (biphenyl-3,3′,5,5′-tetra-(phenyl-4-carboxylate)) ligands in a 1:1 ratio (Scheme 1). Each $[In(O_2CR)_4]$ node connects to four different deprotonated ligands to give a tetrahedral **4-c** center, and vice versa to afford an overall diamondoid network. The desolvated structure has a BET surface area of 2220 m^2 g^{-1} and a large pore void comprising ∼70% of the volume, estimated by PLATON/SOLV.[22]

Scheme 1. Chemical Structure of H_4L Used to Construct the NOTT-202 Frameworks

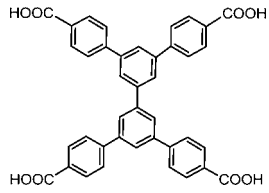

The uptake of SO_2 by desolvated NOTT-202a between 268 and 303 K (Figure 1) confirms that at low pressures the uptake capacities decrease gradually with increasing temperature (Figure S10), consistent with an exothermic sorption mechanism. At increased pressure, however, adsorption of SO_2 at 293, 298, and 303 K reaches saturation at similar uptake capacities of ∼8 mmol g^{-1} at 1.0 bar, giving type-I isotherms. In contrast, adsorption isotherms of SO_2 at 268, 273, and 283 K

Received: January 30, 2013
Published: March 13, 2013

   dx.doi.org/10.1021/ja401061m | J. Am. Chem. Soc. 2013, 135, 4954−4957

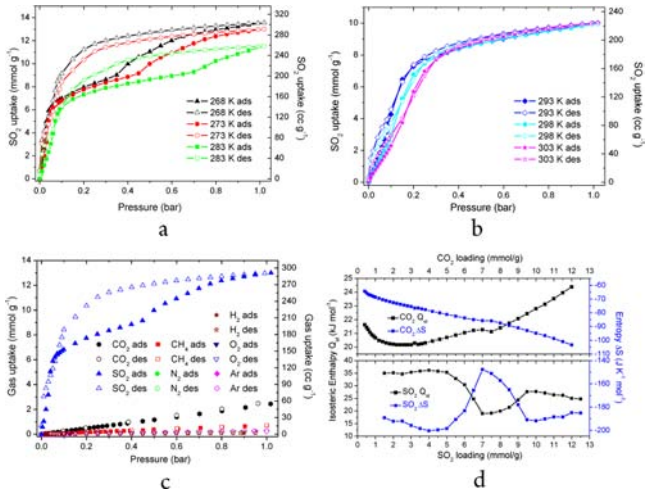

Figure 1. Gas sorption isotherms for NOTT-202a. (a) SO_2 sorption isotherms at 268, 273, and 283 K; (b) SO_2 sorption isotherm at 293, 298, and 303 K; (c) comparisons of ambient pressure SO_2, CO_2, CH_4, N_2, Ar, O_2, and H_2 sorption isotherms at 273 K; (d) variation of thermodynamic parameters Q_{st} and ΔS as a function of CO_2 uptake (top) and SO_2 uptakes (bottom).

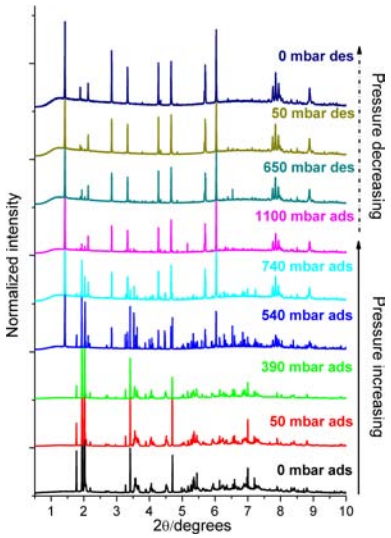

Figure 2. Comparison of *in situ* high resolution powder diffraction patterns for NOTT-202a as a function of different SO_2 loadings, λ = 0.49581 Å.

show inflection points above the plateau uptake of ~8 mmol g^{-1} at 0.35, 0.45, and 0.75 bar, respectively, and a further 2−6 mmol g^{-1} of SO_2 are adsorbed at 1.0 bar, giving two-step isotherm profiles. At 268−283 K, the corresponding desorption isotherms do not follow the adsorption branches, resulting in broad hysteresis loops. At higher temperatures (293−303 K), the second SO_2 uptake step disappears and the corresponding desorption isotherms exhibit good reversibility. A maximum SO_2 uptake of 13.6 mmol g^{-1} (87.0 wt %) was recorded at 268 K and 1.0 bar, representing the highest value observed so far.[19−21] It is important to note that all adsorbed SO_2 is released from this system on returning to $P/P_0 = 0$.

The presence of a stepwise adsorption isotherm coupled with broadly hysteretic desorption behavior is indicative of a potential framework phase transition.[3] To probe this SO_2−host system, *in situ* synchrotron X-ray powder diffraction (PXRD) patterns were recorded for NOTT-202a at 273 K under vacuum and at various SO_2 adsorption pressures (Figure 2). Similar studies were carried out for desorption at pressures of 650 and 50 mbar and under vacuum. The PXRD pattern of freshly desolvated NOTT-202a is consistent with the single crystal structure of NOTT-202a, thus confirming the bulk phase purity. No apparent phase change is observed in the PXRD patterns recorded at SO_2 loadings of 50 and 390 mbar, confirming retention of the crystal structure of NOTT-202a at low SO_2 pressures, where the isotherm is in the first plateau region. At 540 mbar of SO_2 pressure, where the isotherm exhibits the second step, a series of sharp diffraction peaks appears at lower 2θ angle (*e.g.*, 1.40°, 2.80°), suggesting the presence of a new phase (NOTT-202b). However, the diffraction peaks for NOTT-202a are still present at this pressure, indicating that the phase conversion is not complete. With increasing SO_2 pressure, the peaks for NOTT-202a decrease in intensity while those of NOTT-202b increase. This network transformation nearly reaches completion at 1100 mbar of SO_2 where the bulk of the material is now NOTT-202b. Significantly upon desorption and removal of all SO_2 under vacuum, the PXRD pattern and crystal structure of NOTT-202b are retained, confirming that the phase transition of NOTT-202a to NOTT-202b is irreversible. This is quite distinct from previously reported examples of reversible framework breathing upon guest inclusion[3−11] and can be viewed as a high yield (~100%) catalytic reaction, in which NOTT-202a is converted to NOTT-202b in the presence of the SO_2 catalyst.

The PXRD pattern for NOTT-202b was indexed to a monoclinic cell, related to the original structure of NOTT-202-solv (Table S1) but with the *a*-axis being halved. A good Le Bail fitting was obtained in the space group $A2/a$ from the reflection conditions (hkl: $k + l = 2n$; $h0l$: $l = 2n$) (Figure S9). As determined by the isosteric enthalpies (Q_{st}) and entropies (ΔS) of SO_2 adsorption (see below), no significant bond breaking was observed during the SO_2 adsorption, suggesting that the basic framework structure is retained during the phase transformation. The structural model for NOTT-202b was sequentially developed based upon the structure of NOTT-202-solv by putting one network in the unit cell and generating the other one by the operation of the *a*-glide plane. The resultant model is similar to NOTT-202-solv except that the second network is shifted by about **c/4-b/6** in the *bc* plane (Figure 3). In addition, the halved *a*-axis duplicates the network to create two equally occupied positions with half the occupancy for each network, resulting in a highly disordered framework upon SO_2 inclusion. Due to the complexity (50 independent atoms) of the structure, the disorder of the frameworks, and the lack of resolved diffraction peaks, a satisfactory Rietveld refinement model was not obtained. However, the simulated PXRD pattern based on the NOTT-202b model is in good agreement with the experimental PXRD pattern (Figure S8), confirming the reliability of the structural model for NOTT-202b. Disagreement of some *hkl* reflections with $h \neq 0$ is due to the disorder of the network along the *a*-axis. According to the PLATON/VOID[22] calculation, the structural voids in NOTT-202a (before transition, 71%) and NOTT-202b (after transition, 68%) are comparable to each other. Careful examination of the packing of the two networks in NOTT-202a and NOTT-202b shows interesting changes in π...π stacking between the two forms. In NOTT-202a, the phenyl rings on the ligand of two individual networks are in

dx.doi.org/10.1021/ja401061m | *J. Am. Chem. Soc.* 2013, 135, 4954−4957

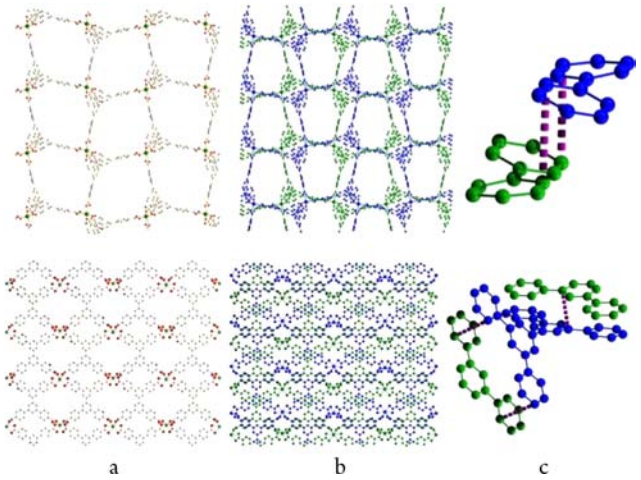

Figure 3. (a) View of the crystal structures for the single network along *a* axis (indium, green; oxygen, red; carbon, gray); (b) view of the crystal structures of doubly interpenetrated frameworks along the *a* axis showing the π...π interactions between two networks (shown in blue and green); (c) detailed view of the π...π stacking between the two independent networks (the π...π interaction is highlighted in purple). All H-atoms are omitted for clarity. Figures in the top row correspond to NOTT-202a, while those in the bottom correspond to NOTT-202b.

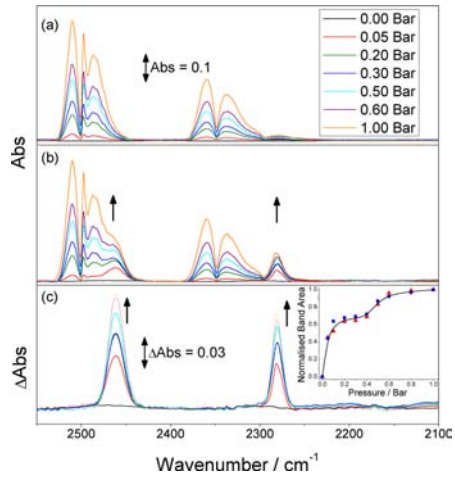

Figure 4. *In situ* DRIFTS spectra of gaseous SO_2 at various pressures (0−1 bar) in the overtone region at 273 K: (a) KBr + SO_2, (b) KBr + NOTT-202a + SO_2, and (c) the difference spectra, showing the growth of two new bands. Arrows indicate the growth of bands due to adsorbed SO_2 with increasing pressure. Inset: Plot showing the growth of the new bands at 2461 (red ▲) and 2280 cm^{-1} (blue ■) as a function of SO_2 pressure. The areas were averaged at each pressure to produce a point-to-point average (black beta-spline line).

completely offset positions (perpendicular distance between planes: 3.70 Å) reflecting weak π...π interactions between networks (Figure 3c). In NOTT-202b, after shifting the secondary network, the phenyl rings on the ligand of two individual networks are in a perfect half-offset position (perpendicular distance between planes: 3.30 Å) to form triple π...π interactions that stabilize the overall framework (Figure 3c). Thus, the formation of relatively strong π...π interactions in NOTT-202b maintains the resultant framework structure against the highly corrosive nature of SO_2 and allows additional SO_2 uptake after the phase transition. Interestingly, Kitagawa *et al.* have recently reported shape-memory phase transition in MOFs stabilized by crystal downsizing.[23] In the case of NOTT-202b, π...π interactions are modulated by SO_2 uptake and stabilize the structure upon removal of SO_2 *via* an irreversible phase transition.

We have probed the SO_2 sorption process in NOTT-202a *via in situ* DRIFTS (Diffuse Reflectance Infrared Fourier Transform Spectroscopy) by monitoring the overtone vibrations of SO_2 in the region 2250−2540 cm^{-1} (Figure 4). Background spectra of SO_2 in the absence of NOTT-202a were collected within a KBr disc, and the two overtone bands observed at *ca.* 2500 and 2350 cm^{-1} were assigned to overtone and combination bands, respectively. A sample of NOTT-202a diluted with KBr was then exposed to increasing pressures of SO_2 gas (0−1 bar) at 273 K, and two new IR bands were observed at 2461 and 2280 cm^{-1} consistent with SO_2 within the porous material. A comparison of the uptake isotherm (Figure 1a) with the integrated areas of these two IR bands (Figure 4c inset) shows good agreement between both experiments, which display a distinctive two-step uptake of SO_2. The IR bands of the local framework also change during adsorption of SO_2 (Figures S1,S2); the major changes in the IR spectra appear between 0.4 and 0.5 bar, consistent with a structural change occurring over this pressure range, as observed by *in situ* PXRD studies.

The isosteric enthalpies (Q_{st}) and entropies (ΔS) of SO_2 adsorption were calculated from the SO_2 isotherms measured at 268−303 K using the van't Hoff isochore (Figure 1d). The isosteric enthalpy Q_{st} (35 kJ mol^{-1}) and entropy ΔS (−190 to −200 J K^{-1} mol^{-1}) of SO_2 adsorption do not change significantly over the uptake range of 1−5 mmol g^{-1}. At higher uptakes, Q_{st} decreases sharply to 19 kJ mol^{-1} and simultaneously ΔS increases rapidly to −147 J K^{-1} mol^{-1} at ∼7 mmol g^{-1}.These changes correspond to a sudden increase in disorder of the SO_2−host system. The free-energy difference (ΔF_{host}) between NOTT-202a and NOTT-202b, estimated using the Langmuir−Freundlich equation combined with a modified thermodynamic model used for other porous MOFs,[24,25] was found to be 20.5 kJ mol^{-1} (Figure S12). This free-energy difference is higher than that observed in [Co(BDP)] (BDP = 1,4-benzenedipyrazolate) (3.3 kJ mol^{-1}),[24] $[Cu(4,4'\text{-bipy})(dhbc)_2]\cdot H_2O$ (4,4′-bipy = 4,4′-bipyridine; dhbc = 2,5-dihydroxybenzoate) (6 kJ mol^{-1}),[24] or MIL-53 (Al, Cr) (2.5 kJ mol^{-1}),[24] indicating a larger difference in relative stabilities of the NOTT-202a and NOTT-202b phases in comparison to these "breathing frameworks". This result is in good agreement with the structural analysis and the irreversible nature of this SO_2-induced phase change to NOTT-202b. The enthalpy of adsorption drives the adsorption process which induces framework disorder above a loading of 5 mmol g^{-1} (stoichiometry 4.0 SO_2/In), with subsequent ordering above the 7 mmol g^{-1} loading inducing the phase change from NOTT 202a to NOTT-202b. When the structural change is complete above an uptake of 9.5 mmol g^{-1}, Q_{st} increases to ∼28 kJ mol^{-1} and ΔS decreases to ∼ −190 J K^{-1} mol^{-1}. The latter value is similar to the values observed before the structural change. The Q_{st} for SO_2 adsorption in NOTT-202b (28 kJ mol^{-1}) is lower than that in NOTT-202a (35 kJ mol^{-1}), consistent with the increased framework stability and porosity in NOTT-202b.

The variation in these thermodynamic parameters for SO_2 adsorption in NOTT-202a contrasts with that observed for CO_2 adsorption. Q_{st} has a relatively narrow range (20−22 kJ

dx.doi.org/10.1021/ja401061m | *J. Am. Chem. Soc.* 2013, 135, 4954−4957

mol^{-1}) for CO_2 uptakes up to 7 mmol g^{-1}, increasing slowly to 25 kJ mol^{-1} at a higher uptake of 12 mmol g^{-1}, while ΔS decreases continuously with increasing surface coverage, corresponding to ordering of the CO_2–host system. In contrast, the adsorption of SO_2 in NOTT-202a results initially in ΔS decreasing slightly before increasing due to disorder of the SO_2–host system with increasing chemical potential (SO_2 pressure): this leads to ordering within the NOTT-202b, which has increased framework stability and total porosity. This difference in thermodynamic parameters for CO_2 and SO_2 uptakes is most likely due to the permanent dipole moment of SO_2 (1.62 D), which results in the pore surface forming stronger electrostatic interactions with SO_2 than with the CO_2, consistent with their values of Q_{st} at zero surface coverage.

In addition to the high uptake capacity of SO_2, NOTT-202a/NOTT-202b also exhibits good selectivity for SO_2 against other gases (*e.g.*, CO_2, N_2, CH_4, O_2). Comparison of a range of gas adsorption isotherms at 273 and 293 K (Figures 1c, S11) clearly shows that NOTT-202a/NOTT-202b can selectively adsorb SO_2 gas, the uptakes at 1.0 bar being 6–130 times greater than those for other gases on a molar basis. Analysis of the selectivity data based upon the Henry Law constants also confirms good selectivity for SO_2 (Table S3).

In conclusion, the adsorption of SO_2 by NOTT-202a at 268–283 K shows two distinct steps with broadly hysteretic desorption coupled to a framework phase change, which have been studied by *in situ* PXRD, *in situ* IR spectroscopy, and detailed thermodynamic analysis. The adsorption is driven by the isosteric enthalpy leading to a structural change involving initial disordering and then reordering to form a new framework structure NOTT-202b. These results indicate that SO_2 adsorption in MOFs may induce new types of framework flexibility and functionality, and by using SO_2 gas as a catalyst, it is possible to uncover new phases of MOFs which cannot be obtained *via* traditional solvothermal synthesis.

■ ASSOCIATED CONTENT

Ⓢ Supporting Information

Experimental details, detailed powder diffraction patterns, additional views of crystal structures, and additional gas adsorption isotherms analysis. This material is available free of charge via the Internet at http://pubs.acs.org.

■ AUTHOR INFORMATION

Corresponding Author

M.Schroder@nottingham.ac.uk; Sihai.Yang@nottingham.ac.uk

Present Address

[#]Johnson Matthey Technology Centre, Savannah, Georgia 31408, United States

Notes

The authors declare no competing financial interest.

■ ACKNOWLEDGMENTS

S.Y. and M.S. gratefully acknowledge receipt of a Leverhulme Trust Early Career Research Fellowship and an ERC Advanced Grant, respectively. We thank EPSRC for support and Diamond Light Source and the European Synchrotron Radiation Facility (ESRF) for access to Beamlines I11 and ID31, respectively. J.S. acknowledges support from the Swedish Research Council (VR). M.W.G. gratefully acknowledges receipt of a Royal Society Wolfson Merit award. We thank Harrick Scientific Products Inc. for the loan of a Harrick Praying Mantis and a diffuse reflectance high temperature chamber and Dr. Jeffery Christenson (Harrick) for helpful discussions.

■ REFERENCES

(1) Zhang, J.; Chen, S. M.; Zingiryan, A.; Bu, X. H. *J. Am. Chem. Soc.* **2008**, *130*, 17246.

(2) Long, J. R.; Yaghi, O. M. *Chem. Soc. Rev.* **2009**, *38*, 1201. Lin, X.; Champness, N. R.; Schröder, M. *Top. Curr. Chem.* **2010**, *293*, 35.

(3) Férey, G.; Serre, C. *Chem. Soc. Rev.* **2009**, *38*, 1380.

(4) Serre, C.; Mellot-Draznieks, C.; Surble, S.; Audebrand, N.; Filinchuk, Y.; Férey, G. *Science* **2007**, *315*, 1828.

(5) Serre, C.; Bourrelly, S.; Vimont, A.; Ramsahye, N. A.; Maurin, G.; Llewellyn, P. L.; Daturi, M.; Filinchuk, Y.; Leynaud, O.; Barnes, P.; Férey, G. *Adv. Mater.* **2007**, *19*, 2246.

(6) Millange, F.; Serre, C.; Guillou, N.; Férey, G.; Walton, R. I. *Angew. Chem., Int. Ed.* **2008**, *47*, 4100.

(7) Boutin, A.; Springuel-Huet, M. A.; Nossov, A.; Gedeon, A.; Loiseau, T.; Volkringer, C.; Ferey, G.; Coudert, F. X.; Fuchs, A. H. *Angew. Chem., Int. Ed.* **2009**, *48*, 8314.

(8) Salles, F.; Maurin, G.; Serre, C.; Llewellyn, P. L.; Knofel, C.; Choi, H. J.; Filinchuk, Y.; Oliviero, L.; Vimont, A.; Long, J. R.; Férey, G. *J. Am. Chem. Soc.* **2010**, *132*, 13782.

(9) Henke, S.; Schneemann, A.; Wuetscher, A.; Fischer, R. A. *J. Am. Chem. Soc.* **2012**, *134*, 9464.

(10) Yang, C.; Wang, X. P.; Omary, M. A. *Angew. Chem., Int. Ed.* **2009**, *48*, 2500.

(11) Horike, S.; Shimomura, S.; Kitagawa, S. *Nat. Chem.* **2009**, *1*, 695.

(12) Yang, W.; Davies, A. J.; Lin, X.; Suyetin, M.; Matsuda, R.; Blake, A. J.; Wilson, C.; Lewis, W.; Parker, J. E.; Tang, C. C.; George, M. W.; Hubberstey, P.; Kitagawa, S.; Sakamoto, H.; Bichoutskaia, E.; Champness, N. R.; Yang, S.; Schröder, M. *Chem. Sci.* **2012**, *3*, 2993.

(13) Mulfort, K. L.; Farha, O. K.; Malliakas, C. D.; Kanatzidis, M. G.; Hupp, J. T. *Chem.—Eur. J.* **2010**, *16*, 276.

(14) Seo, J.; Matsuda, R.; Sakamoto, H.; Bonneau, C.; Kitagawa, S. *J. Am. Chem. Soc.* **2009**, *131*, 12792.

(15) Yang, S.; Lin, X.; Blake, A. J.; Walker, G. S.; Hubberstey, P.; Champness, N. R.; Schröder, M. *Nat. Chem.* **2009**, *1*, 487.

(16) Yang, S.; Lin, X.; Lewis, W.; Suyetin, M.; Bichoutskaia, E.; Parker, J. E.; Tang, C. C.; Allan, D. R.; Rizkallah, P. J.; Hubberstey, P.; Champness, N. R.; Thomas, K. M.; Blake, A. J.; Schröder, M. *Nat. Mater.* **2012**, *11*, 710.

(17) Ehhalt, D. H. *Phys. Chem. Chem. Phys.* **1999**, *1*, 5401.

(18) Vahedpour, M.; Zolfaghari, F. *Struct. Chem.* **2011**, *22*, 1331.

(19) Thallapally, P. K.; Motkuri, R. K.; Fernandez, C. A.; McGrail, B. P.; Behrooz, G. S. *Inorg. Chem.* **2010**, *49*, 4909.

(20) Yang, S.; Sun, J.; Ramirez-Cuesta, A. J.; Callear, S. K.; David, W. I. F.; Anderson, D. P.; Newby, R.; Blake, A. J.; Parker, J. E.; Tang, C. C.; Schröder, M. *Nat. Chem.* **2012**, *4*, 887.

(21) Fernandez, C. A.; Thallapally, P. K.; Motkuri, R. K.; Nune, S. K.; Sumrak, J. C.; Tian, J.; Liu, J. *Cryst. Growth Des.* **2010**, *10*, 1037.

(22) Spek, A. L. *Acta Crystallogr., Sect. D* **2009**, *65*, 148.

(23) Sakata, Y.; Furukawa, S.; Kondo, M.; Hirai, K.; Horike, N.; Takashima, Y.; Uehara, H.; Louvain, N.; Meilikhov, M.; Tsuruoka, T.; Isoda, S.; Kosaka, W.; Sakata, O.; Kitagawa, S. *Science* **2013**, *339*, 193.

(24) Coudert, F.-X.; Jeffroy, M.; Fuchs, A. H.; Boutin, A.; Mellot-Draznieks, C. *J. Am. Chem. Soc.* **2008**, *130*, 14294.

(25) Wang, Z.; Cohen, S. M. *J. Am. Chem. Soc.* **2009**, *131*, 16675.